CRACK ANALYSIS OF CONCRETE BEAMS BASED ON PSEUDO-DISCRETE CRACK MODEL

P.L. Ng [1,2*], F.J. Ma [1] and A.K.H. Kwan [1]
[1] Department of Civil Engineering, The University of Hong Kong, Pokfulam, Hong Kong, China
[2] Faculty of Civil Engineering, Vilnius Gediminas Technical University, Vilnius, Lithuania
*Email: irdngpl@gmail.com

ABSTRACT

Crack widths are important considerations in both serviceability and durability design of concrete structures and should be evaluated to ensure compliance with design limits. However, existing empirical formulas for maximum crack width prediction are discrepant with each other, and they cannot reveal key information such as crack number and crack spacing. To obtain such information, finite element analysis has to be adopted. However, conventional finite element analysis has its limits in carrying out crack analysis. Particularly, the common smeared crack models, which do not realistically reflect bond-slip of reinforcing bars, would not give correct crack widths. In contrast, the discrete crack models are difficult to apply because of the need to adaptively generate discrete crack elements according to the cracks formed during the loading process. In this paper, a pseudo-discrete crack model is developed for finite element implementation. The conventional smeared crack model is transformed and reformulated, and a novel crack queuing algorithm is introduced for crack analysis. The method has been applied to analyse concrete beams in the literature. It is demonstrated that the computational results of crack number, spacing and widths agree closely with the measured results.

KEYWORDS

Crack width, crack queuing algorithm, pseudo-discrete crack model, finite element analysis.

INTRODUCTION

In the design of reinforced concrete structures, crack width is a major factor to be considered, and has to be limited to a certain maximum allowable value to ensure the serviceability and durability performance. However, only empirical formulas for crack width prediction are given in design codes, such as British Standard BS 8110, American Concrete Institute ACI 224R-01, and Eurocode 2, and these formulas do not agree with each other. One probable reason is that the phenomena of crack initiation, propagation and widening are fairly complicated and difficult to analyse. Specialised numerical techniques are required to deal with the stress concentrations at crack tips, stress redistribution during crack formation, and bond-slip of steel reinforcing bars when cracks widen. Hence, conventional finite element methods have limited capability in analysing the crack number, spacing and widths in concrete.

Finite element methods for concrete cracking simulation may be categorized into discrete crack model and smeared crack model. The discrete crack model was first proposed by Ngo and Scordelis (1967) where the crack location was predetermined, also by Nilson (1968) where crack propagation was restricted to follow the boundaries of finite elements. Adaptive insertion of discrete crack elements according to the analytical stress field could lead to more realistic crack patterns (Hillerborg et al. 1976; Ingraffea and Saouma 1985; Bittencourt et al. 1996), but this requires re-meshing in each iteration step (Yang and Chen 2005). Such would incur high demand of computational resources and rendering the adaptive discrete crack model difficult to apply.

Rashid (1968) was among the earliest researchers who developed the smeared crack model, in which the formation of a crack is simulated by altering constitutive properties of the concrete element containing the crack, i.e. the crack is in effect smeared within the volume of concrete element. The smeared crack model may be further categorized into the non-rotating crack model (Rashid 1968; Suidan and Schnobrich 1973; Cervenka 1985) and rotating crack model (De Borst and Nauta 1985; Willam et al. 1987). In the non-rotating crack model, the crack directions are assumed to be fixed once the cracks are formed but in the rotating crack model, the cracks are allowed to rotate with the principal strain directions. However, in most smeared crack models, the steel reinforcing bars are also smeared within the concrete element (Cope et al. 1980; Gupta and Akbar 1984). As a result, the bond-slip of the steel reinforcing bars, which has great influence on the crack width, is ignored.

To predict the crack number, spacing and widths, accounting for the bond-slip of reinforcing bars is not a sufficient condition. Since there would be stress concentration at crack tips, the fracture toughness of concrete needs to be considered. Moreover, during crack formation and propagation, there would be immediate stress redistribution in the vicinity of cracks, which would relieve the tensile stresses normal to the cracks to elude the formation of other cracks close to the newly formed cracks. In conventional finite element methods, stress relief is not taken into account and consequently, many false cracks which should not exist in reality are often generated. Herein, a pseudo-discrete crack model taking into account the stress concentration and fracture toughness in the cracking criteria is developed, and stress relief upon crack formation is simulated using a novel crack queuing algorithm, which allows only one crack to form at a time and evaluating the stress redistribution so caused by re-analysing the concrete stresses before allowing another crack to form. Through transforming and reformulating the smeared crack model, the pseudo-discrete crack model successfully circumvents the difficulty in applying the discrete crack model.

MODELLING STRATEGIES BY FINITE ELEMENT METHOD

The proposed discrete crack model was implemented in a nonlinear finite element programme developed by the authors. In this section, the basic assumptions and methodologies of modelling are stated. The sign convention adopted is tension positive and compressive negative. At each load increment step, direct iteration based on secant stiffness is performed.

Concrete Elements

The concrete is modelled by 3-noded triangular elements, which is allowed to have tensile cracks formed inside the element. To cater for the nonlinear behaviour, the biaxial stress-strain relations in the local coordinates are transformed into two uniaxial stress-strain relations such that each of the two axial stresses is taken as a function of the equivalent uniaxial strain in that direction (Wang et al. 1999; Kwan et al. 1999; Ng 2007). The equivalent uniaxial strains, denoted by ε_1^e and ε_2^e, are defined by Equations (1) and (2), in which ε_1 and ε_2 are the axial strains in the local coordinates, and ν_1 and ν_2 are the Poisson's ratios.

$$\varepsilon_1^e = \frac{1}{1-\nu_1\nu_2}\left(\varepsilon_1 + \nu_2\varepsilon_2\right) \tag{1}$$

$$\varepsilon_2^e = \frac{1}{1-\nu_1\nu_2}\left(\varepsilon_2 + \nu_1\varepsilon_1\right) \tag{2}$$

When the equivalent uniaxial strain is compressive, the stress-strain curve developed by Desayi and Krishnan (1964) is used. Under tension, the concrete is assumed to be linearly elastic before cracking and have no tensile capacity after cracking as adopted in the elasto-plastic analyses by Kwan et al. (1998). To account for the biaxial behaviour, the biaxial strength envelope developed by Kupfer and Gerstle (1973) is adopted.

Regarding the cracking criteria, if there is no crack tip nearby a concrete element, it is assumed that the concrete would crack when the tensile stress exceeds the tensile strength. On the other hand, if there is a crack tip nearby, both the tensile strength and fracture toughness are considered, as will be elucidated in the subsequent section. Once cracks are formed, the crack directions are fixed. In other words, the non-rotating crack model is adopted.

Rebar Elements

The reinforcing bars are separately modelled by discrete rebar elements. It is because the crack width is largely dependent on the bond-slip between reinforcing bar and concrete. Each rebar element has 2 nodes having the same coordinates as the nodes of the concrete elements to which the rebar element is connected, but the nodes on the steel bar element can have different displacements from those of the concrete elements so as to allow for bond-slip. For the constitutive modelling, the steel reinforcing bars are assumed to be linearly elastic and plastic with strain hardening (Mander 1983).

Rebar-Concrete Interface Elements

To allow for bond-slip between reinforcing steel and concrete, interface elements with 2 connection points and 4 nodes are inserted between the rebar elements and the concrete elements (Goodman et al. 1968; Ng et al. 2011; Kwan and Ng 2013). At each connection point there are paired nodes and a shear spring to simulate the bond stress-slip relation, which refers to CEB-FIP Model Code 1990. The bond-slip at a connection point is calculated as the difference in longitudinal displacements of the 2 nodes there, and the stiffness of shear spring

at the connection point is evaluated as the bond stiffness times the perimeter of the steel reinforcing bars times half of the length of interface element. It is noteworthy to point out that as the bond-slip will change direction across a crack (this will be explicated in detail later), the interface elements should be formulated using discrete shear springs as proposed by the authors, rather than using continuous shear springs (Keuser and Mehlhorn 1987; Jendele and Cervenka 2006).

IMPLEMENTATION OF PSEUDO-DISCRETE CRACK MODEL

A number of specialised numerical techniques have been devised for the implementation of pseudo-discrete crack model, as detailed in the following sections.

Crack Queuing Algorithm

Upon the formation of a crack, there would be stress redistribution and the tensile stress perpendicular to the crack would be relieved thereby eluding the formation of other cracks in the vicinity. The stress redistribution has to be accounted for by re-analysing the concrete stresses before allowing any other cracks to be formed. Otherwise, false cracks caused by numerical instability would appear upon the exertion of a load increment, and erroneous computed crack pattern, crack spacing and crack widths would result. This necessitates the crack queuing algorithm (Kwan et al. 1999), which is first introduced herein to the pseudo-discrete crack model.

At each loading step, the concrete element with the highest tensile stress to tensile strength ratio is searched. If the ratio is less than 1.0, no new crack is formed and the analysis can proceed to the next load increment step. Otherwise, if the ratio is equal to or higher than 1.0, only this concrete element is allowed to crack, and its stiffness matrix is altered to reflect the crack formation. Then, the whole concrete structure is re-analysed with the same loading level so as to cater for the stress redistribution. This process is repeated until no more new crack is formed after re-analysis, the analysis proceeds to the next loading step. Using this crack queuing algorithm, the crack pattern so obtained would contain genuine cracks with realistic crack widths.

Fracture Toughness

Near crack tips, there is occurrence of stress concentration (Griffith 1920) and if very fine element mesh is used, the tensile stresses obtained in the concrete elements in front of and close to crack tips can be much higher than the tensile strength of concrete. If the tensile strength is solely adopted as the cracking criterion, the crack pattern obtained would be mesh size dependent and the crack propagation would be very rapid and unstable. In order to avoid the mesh size dependence and stabilise the crack propagation, the fracture toughness K_{IC} is incorporated as a cracking criterion.

According to Erdogan and Sih (1963), crack propagation initiates when $\sigma_\theta(2\pi r)^{0.5} \geq K_{IC}$, in which σ_θ is the circumferential stress (the stress perpendicular to the line joining the point being considered to the crack tip) and r is the distance from the point being considered to the crack tip. In graphical representation, the stress field near a crack tip in polar coordinates is illustrated in Figure 1, where r and θ are the polar coordinates with the crack tip as the origin. Mathematically, the criterion may be written as:

$$\sigma_\theta \geq \frac{K_{IC}}{\sqrt{2\pi r}} \tag{3}$$

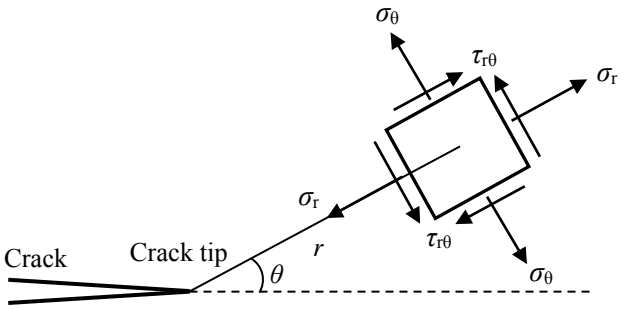

Figure 1 Stress field near crack tip in polar coordinates

In actual application, for each concrete element being considered, a search is conducted to find out if there is any crack tip in the adjoining concrete elements, i.e. concrete elements having one or more common nodes with the concrete element being considered. If there is any crack tip in any of the adjoining concrete elements, the distance r is determined as the distance from the centroid of the concrete element being considered to the centroid of the concrete element containing the crack tip. Having determined the distance r, the cracking criterion for the concrete element being considered is modified as maximum tensile stress exceeding the equivalent tensile strength f_t^e, which is taken as the maximum of $K_{IC}/(2\pi r)^{0.5}$ and tensile strength of concrete f_t. With this modified cracking criterion, the crack propagation would remain stable even when a very fine mesh is used in the finite element analysis.

Crack Width Calculation

For a concrete element which is cracked, the crack is assumed to be formed at the centroid of element and non-rotating. After re-analysis to allow for stress redistribution due to formation of the crack, the tensile stress in the direction perpendicular to the crack would drop to a negligibly small value, which may be assumed as zero. Based on this assumption, the crack width can be calculated from the nodal displacements of the cracked concrete element.

As shown in Figure 2, the crack through the centroid would separate the concrete element into two portions, each at one side of the crack. Denote the 3 nodes of concrete element by I, J and K, in such a manner that node I is the node closest to the crack and nodes J and K are at opposite sides of the crack (node J and K are always belonging to different portions of the concrete element), and further denote the crack angle (the angle between the normal direction of the crack and the x-axis) by α. The displacement of node J from the crack d_J and the displacement of node K from the crack d_K may be computed as:

$$d_J = -u_J \cos\alpha - v_J \sin\alpha \tag{4}$$

$$d_K = u_K \cos\alpha + v_K \sin\alpha \tag{5}$$

in which u_J and v_J are the nodal displacements of node J in the x- and y-directions, and u_K and v_K are the nodal displacements of node K in the x- and y-directions. From these displacements, the crack width w can be calculated from Equation (6). It should be noted that the absolute value is taken because the nodes J and K may swap in position leading to negative value of their relative displacement from the crack.

$$w = | d_J + d_K | \tag{6}$$

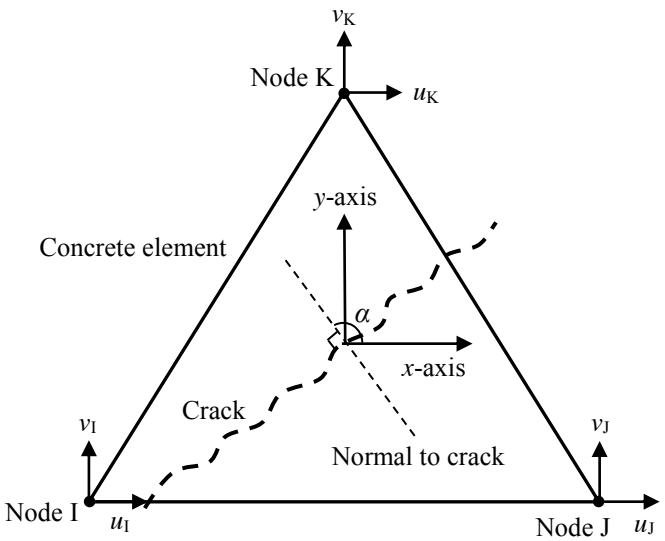

Figure 2 Calculation of crack width

APPLICATIONS TO CONCRETE BEAM ANALYSIS

Beam Specimens Analysed

To evaluate the applicability and accuracy of the finite element analyses incorporating the pseudo-discrete crack model, 19 nos. reinforced concrete beam specimens tested by Clark (1956) are analysed and compared with the experimental results. All these beams have a total length of 3353 mm and a span length of 2743 mm. They have an uniform cross-section of 381 mm depth by 152 mm width. The longitudinal reinforcement ratio varied from 1.01% to 2.58%. No stirrups were provided. All the beams were subjected to two-point loading and the loading points were spaced 1372 mm apart symmetrically, as shown in Figure 3. The beams are designated by beam number in the form of A-B-C-D, where A is the depth of section (in inches), B is the width of section (in inches), C is the bar size number and D is a serial number, as listed in Table 1.

Table 1 Details of beam specimens tested by Clark (1956)

Beam number	Rebar diameter (mm)	No. of rebars	Effective depth (mm)	Reinforce-ment ratio (%)	Concrete strength (MPa)
15-6-8-1	25.4	1	330.2	1.01	26.8
15-6-8-2	25.4	1	330.2	1.01	25.9
15-6-6-1	19.1	2	339.9	1.10	30.1
15-6-6-2	19.1	2	339.9	1.10	29.2
15-6-6-3	19.1	2	333.5	1.12	27.2
15-6-7-1	22.2	2	357.1	1.42	26.8
15-6-7-2	22.2	2	331.7	1.53	22.4
15-6-7-3	22.2	2	331.7	1.53	29.5
15-6-7-4	22.2	2	331.7	1.53	29.0
15-6-7-5	22.2	2	331.7	1.53	27.9
15-6-10-1	32.3	1	326.6	1.65	24.6
15-6-10-2	32.3	1	326.6	1.65	28.7
15-6-8-3	25.4	2	330.2	2.03	26.6
15-6-8-4	25.4	2	330.2	2.03	26.7
15-6-9-1	28.7	2	344.4	2.46	28.1
15-6-9-2	28.7	2	328.7	2.58	28.6
15-6-9-3	28.7	2	328.7	2.58	27.2
15-6-9-4	28.7	2	328.7	2.58	28.6
15-6-9-5	28.7	2	328.7	2.58	24.4

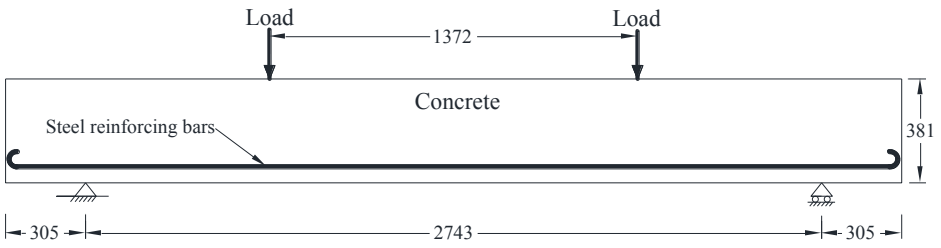

Figure 3 Details of concrete beam (dimensions in mm)

The material properties of the beams are summarised in Table 2. For concrete, the compressive strengths reported by Clark (1956) are used in the analysis. The corresponding range of concrete compressive strengths is stated in Table 2. Since the tensile strengths and initial elastic moduli of concrete were not given by Clark, values calculated based on the reported compressive strengths using the formulas given in American Concrete Institute ACI 318R-02 are used in analysis and stated in Table 2. The Poisson's ratio is assumed to be 0.2 for all concrete. The fracture toughness of concrete was also not presented by Clark, thus the value obtained by Chen et al. (2011) for similar concrete is used.

Table 2 Materials properties of beam specimens

Concrete	
Uniaxial compressive strength (MPa)	22.4-30.1
Uniaxial tensile strength (MPa)	2.6-3.1
Initial elastic modulus (GPa)	22.4-26.0
Poisson's ratio	0.20
Fracture toughness ($MNm^{-2/3}$)	1.26
Steel reinforcement	
Yield strength (MPa)	275.7
Ultimate tensile strength (MPa)	482.6
Initial elastic modulus (GPa)	200.0
Tensile strain at start of strain hardening (%)	1.0
Ultimate tensile strain (%)	10.0
Rebar-concrete bond	
Peak bond stress (MPa)	9.5-11.1
Slip at start of peak bond stress (mm)	0.6
Slip at end of peak bond stress (mm)	0.6
Slip at start of residual bond stress (mm)	2.5
Residual bond stress (MPa)	1.43-1.67

For the steel reinforcing bars, the yield strength and ultimate tensile strength reported by Clark (1956) are used in the analysis. The initial elastic modulus, tensile strain at start of strain hardening and ultimate tensile strain were not reported and are assumed to be 200 GPa, 1% and 10%, respectively. For bond between rebar and concrete, the parameters for bond stress-slip relation are taken from CEB-FIP Model Code 1990. Since no stirrups were provided, the parameters corresponding to unconfined concrete are used in the analysis.

Each reinforced concrete beam is discretized into 13×112 concrete elements, 112 rebar elements along the same line, and 112 interface element also along the same line. The loading is applied in the form of prescribed displacements at the two loading points. In other words, the loading is applied under displacement control.

Results and Discussions

From the finite element analysis results, the crack locations and the variations of steel stress and bond-slip of the reinforcing bars of a typical beam 15-6-8-1 after the formation of the first three cracks are plotted in Figure 4. It is found that the first three cracks were formed at almost the same time. Moreover, the analytical spacing and pattern of the first three cracks agree very well with the spacing and pattern obtained experimentally by Clark (1956). The crack spacing and pattern have been obtained for the other beams, and are found to be in close agreement with the experimental results presented by Clark in all case. Hence, the proposed pseudo-discrete crack model is capable of reproducing the crack patterns of concrete beams.

From the variation of steel stresses plotted in Figure 4(a), it can be seen that the steel stress varies along the rebar with a certain peak value at every crack location. This is because right at a crack, the tension induced by flexure is taken solely by the reinforcing bars but between cracks, the tension induced by flexure is shared amongst the reinforcing bars and the uncracked concrete bonded thereto. Furthermore, from the variation of bond-slip along the reinforcement plotted in Figure 4(b), it is evident that the bond-slip changes direction at every crack. Basically, at the left side of a crack, the reinforcing bars slip towards the right (or the concrete slips towards to left), and vice versa. In other words, the reinforcing bars are always pulling the concretes at the two sides of the crack together so as to limit the crack width while the concretes at the two sides of the crack tend to slip away from the crack (Ng et al. 2010; Lam et al. 2010). In view of the abrupt change in direction of bond-slip at a crack, therefore, discrete shear springs were adopted to formulate the interface elements.

The photograph of experimentally obtained crack pattern reported by Clark (1956) and the analytical crack pattern at yielding of tension reinforcement of beam 15-6-8-1 are presented in Figures 5(a) and 5(b) respectively. It can be seen that the experimental and analytical crack patterns agree well with each other, albeit the presence of random factors in cracking behaviour to a certain extent. Minor non-symmetry in crack trajectories is noted for the analytical crack pattern. This might be due to numerical problems. As an amelioration measure, refinement of load increment steps during the execution of crack queuing algorithm is recommended for further research.

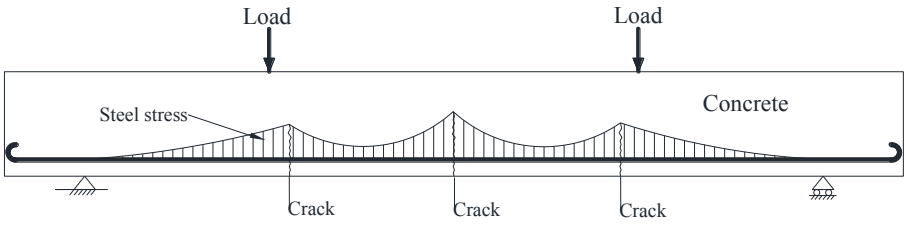

(a) Steel stress

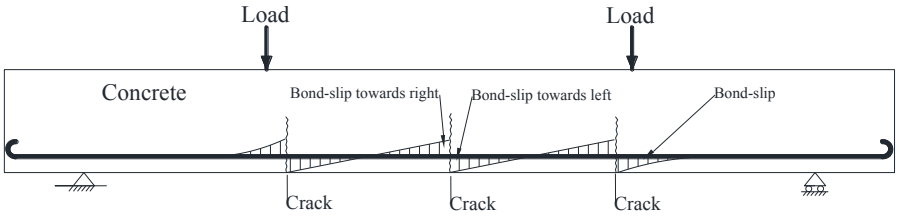

(b) Bond-slip

Figure 4 Variations of steel stress and bond-slip in beam 15-6-8-1 after formation of 3 cracks

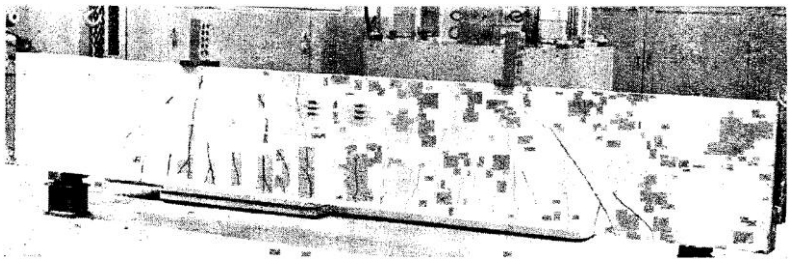

(a) Crack pattern obtained from experiment (Clark 1956)

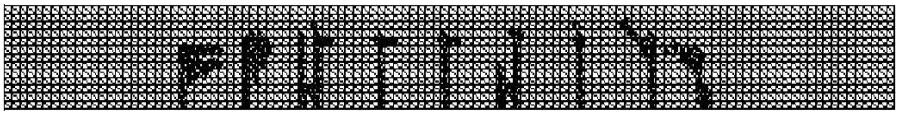

(b) Crack pattern obtained from analysis

Figure 5 Crack pattern of beam 15-6-8-1 at yielding of tension reinforcement

For the reason that the maximum crack width governs the serviceability design, the maximum crack widths but not individual crack widths were reported by Clark (1956). Hereunder, the maximum crack widths obtained from finite element analyses are compared to the experimental results. The 19nos. beam specimens are divided into 4 groups generally according to their reinforcement ratios. The maximum crack width of each beam in these 4 groups is plotted against the steel stress at the widest crack in Figures 6 to 9.

Figure 6 plots the crack widths of beams with reinforcement ratio of 1.0 to 1.1%. In general, when the steel stress is lower than 150 MPa, the analysis overestimated the crack widths. While at higher steel stress level, the analytical crack widths resembled more closely the measured crack widths. Figure 7 plots the crack widths of beams with reinforcement ratio of 1.4 to 1.5%. At steel stress lower than 150 MPa, the analytical crack widths were generally slightly larger than the measured values but at higher steel stress levels, the analytical crack widths became in general slightly smaller than the measured values. Figure 8 plots the crack widths of beams with reinforcement ratio of 1.7 to 2.0%. The analytical crack widths generally agreed very well with the measured results. For beam 15-6-8-3, there was an abrupt increase of measured crack width when the steel stress increased beyond 240 MPa, such might be due to experimental errors. Finally, Figure 9 plots the crack widths of beams with reinforcement ratio of 2.5 to 2.6%. The analytical crack widths were initially slightly larger than the measured values, as the steel stress increased, the analytical crack widths became slightly smaller than the measured values.

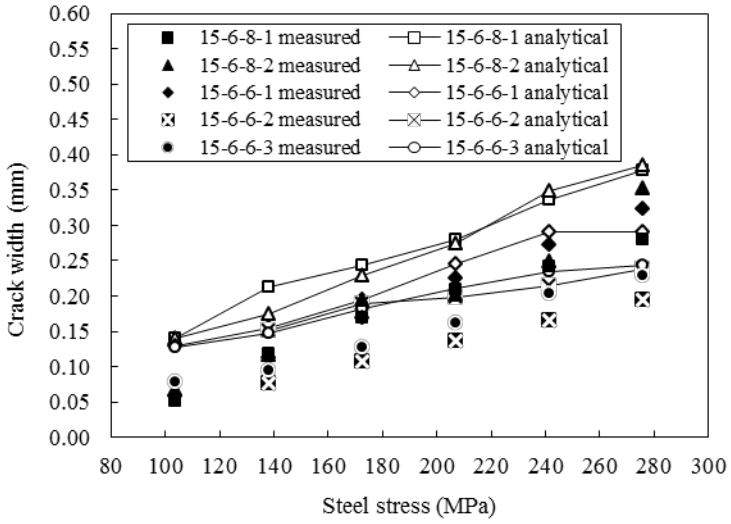

Figure 6 Analytical and measured crack width of beams 15-6-8-1, 15-6-8-2, 15-6-6-1, 15-6-6-2 and 15-6-6-3

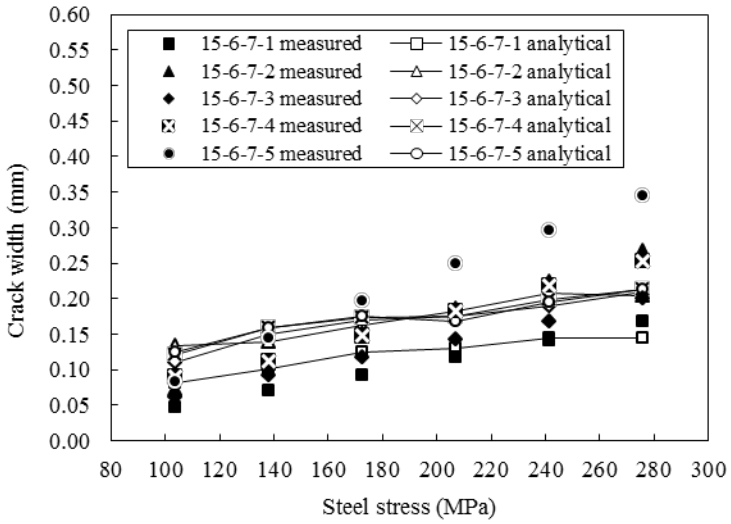

Figure 7 Analytical and measured crack width of beams 15-6-7-1, 15-6-7-2, 15-6-7-3, 15-6-7-4 and 15-6-7-5

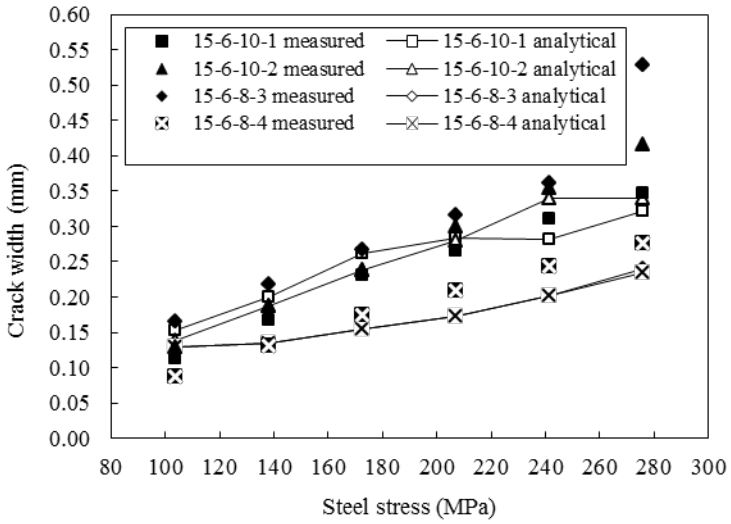

Figure 8 Analytical and measured crack width of beams 15-6-10-1, 15-6-10-2, 15-6-8-3 and 15-6-8-4

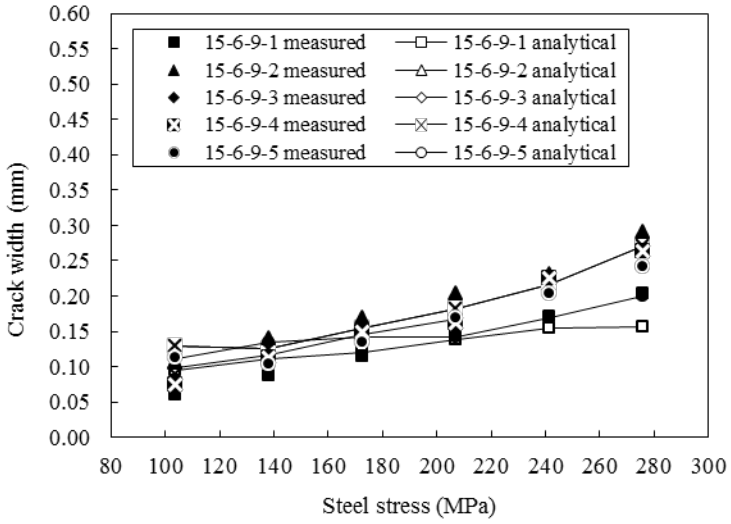

Figure 9 Analytical and measured crack width of beams 15-6-9-1, 15-6-9-2, 15-6-9-3, 15-6-9-4 and 15-6-9-5

The increase in maximum crack width and crack numbers with the steel stress level was studied. From the analytical results, it is observed that for a beam with relatively small number of bars or low reinforcement ratio, the crack number would increase more slowly but the crack width would increase more rapidly with the steel stress. Whereas for a beam with relatively large number of bars or high reinforcement ratio, the crack number would increase more rapidly but the crack width would increase more slowly with the steel stress. The pseudo-discrete crack model presented herein provides a useful tool for investigating the effects of various structural parameters on the cracking behaviour.

CONCLUSIONS

A new pseudo-discrete crack modelling technique for crack analysis of reinforced concrete members by the finite element method has been developed. Discrete rebar elements have been employed to model the reinforcing bars and interface elements incorporating discrete shear springs have been employed to model the bond between rebars and concrete. Specialised numerical techniques have been devised to overcome the difficulties in generating the discrete crack pattern and calculating the crack width: (1) a crack queuing algorithm of allowing only one crack to form at each iteration step so as to cater for the stress redistribution due to formation of new crack before allowing another crack to form; (2) a concrete cracking criterion incorporating both the tensile strength and fracture toughness of concrete in order to avoid mesh size dependence and unstable crack growth due to the stress concentration at crack tips; and (3) a simple method of calculating the crack width from the nodal displacements of the concrete element containing the crack. To verify the applicability and accuracy of the pseudo-discrete crack model, reinforced concrete beams tested in the literature have been analysed for cross-comparison. It has been demonstrated that the analytical crack pattern, numbers and spacing all agree closely with the experimental results.

REFERENCES

Bittencourt, T.N., Wawrzynek, P.A., Ingraffea, A.R. and Sousa, J.L. (1996). "Quasi-automatic simulation of crack propagation for 2D LEFM problems". *Engineering Fracture Mechanics*, 55(2), 321-334.

Červenka, V. (1985). "Constitutive model for cracked reinforced concrete". *ACI Journal*, 82(6), 877-882.

Chen, H.H., Su, R.K.L. and Kwan, A.K.H. (2011). "Fracture toughness of plain concrete made of crushed granite aggregate". *Transactions, Hong Kong Institution of Engineers*. 118(2), 6-12.

Clark, A.P. (1956). "Cracking in reinforced concrete flexural members". *ACI Journal*, 52(4), 851-862.

Cope, R.J., Rao, P.V., Clark, L.A. and Norris, P. (1980). "Modelling of reinforced concrete behavior for finite element analysis of bridge slabs". In *Numerical Methods for Non-linear problems*, Pineridge Press, Swansea, UK, 457-470.

De Borst, R. and Nauta, P. (1985). "Non-orthogonal cracks in a smeared finite element model". *Engineering Computations*, 2(1), 35-46.

Desayi, P. and Krishnan, S. (1964). "Equation for the stress-strain curve of concrete". *ACI Journal*, 61(3), 345-350.

Erdogan, F. and Sih, G.C. (1963). "On the crack extension in plates under plane loading and transverse shear". *Journal of Basic Engineering*, ASME, 85(4), 519-525.

Goodman, R.E., Taylor, R.L. and Brekke, T.L. (1968). "A model for the mechanics of jointed rock". *Journal of Soil Mechanics and Foundation Division*, ASCE, 94(3), 637-659.
Griffith, A.A. (1920). "The phenomena of rupture and flow in solids". *Philosophical Transactions of the Royal Society of London*, *Series A*, 221, 163-198.
Gupta, A.K. and Akbar, H. (1984). "Cracking in reinforced concrete analysis". *Journal of Structural Engineering*, ASCE, 110(8), 1735-1746.
Hillerborg, A., Modéer, M. and Petersson, P. (1976). "Analysis of crack formation and crack growth in concrete by means of fracture mechanics and finite elements". *Cement and Concrete Research*, 6(6), 773-781.
Ingraffea, A.R. and Saouma, V. (1985). "Numerical modeling of discrete crack propagation in reinforced and plain concrete". In *Fracture Mechanics of Concrete: Structural Application and Numerical Calculation*. *Vol. 4*. Springer Netherlands, 171-225.
Jendele, L. and Červenka, J. (2006). "Finite element modelling of reinforcement with bond". *Computers and Structures*, 84(28), 1780-1791.
Keuser, M. and Mehlhorn, G. (1987). "Finite element models for bond problems". *Journal of Structural Engineering*, ASCE, 113(10), 2160-2173.
Kupfer, H.B. and Gerstle, K.H. (1973). "Behavior of concrete under biaxial stresses". *Journal of Engineering Mechanics Division*, ASCE, 99(4), 853-866.
Kwan, A.K.H., Dai, H. and Cheung, Y.K. (1998). "Elasto-plastic analysis of reinforced concrete slit shear walls". *Proceedings of the Institution of Civil Engineers, Structures and Buildings*, 128(4), 342-350.
Kwan, A.K.H. and Ng, P.L. (2013). "Modelling dowel action of discrete reinforcing bars for finite element analysis of concrete structures". *Computers and Concrete*, 12(1), 19-36.
Kwan, A.K.H., Wang, Z.M. and Chan, H.C. (1999). "Mesoscopic study of concrete II: nonlinear finite element analysis". *Computers and Structures*, 70(5), 545- 556.
Lam, J.Y.K., Ng, P.L. and Kwan, A.K.H. (2010). "Tension stiffening in reinforced concrete beams: Part 2 - Section and member analysis". *Proceedings of the Institution of Civil Engineers, Structures and Buildings*, 163(1), 29-39.
Mander, J. B. (1983). *Seismic Design of Bridge Piers*, Ph.D. Thesis, University of Canterbury, New Zealand.
Ng, P.L. (2007). *Constitutive Modelling and Finite Element Analysis of Reinforced Concrete Structures*, Ph.D. Thesis, The University of Hong Kong, Hong Kong, 422pp.
Ng, P.L., Lam, J.Y.K. and Kwan, A.K.H. (2010). "Tension stiffening in concrete beams: Part 1 - FE analysis". *Proceedings of the Institution of Civil Engineers, Structures and Buildings*, 163(1), 19-28.
Ng, P.L., Lam, J.Y.K. and Kwan, A.K.H. (2011). "Effects of concrete-to-reinforcement bond and loading conditions on tension stiffening". *Procedia Engineering*, 14, 704-714.
Ngo, D. and Scordelis, A.C. (1967). "Finite element analysis of reinforced concrete beams". *ACI Journal*, 64(3), 152-163.
Nilson, A.H. (1968). "Nonlinear analysis of reinforced concrete by the finite element method". *ACI Journal*, 65(9), 757-766.
Rashid, Y.R. (1968). "Ultimate strength analysis of prestressed concrete pressure vessels". *Nuclear Engineering and Design*, 7(4), 334-344.
Suidan, M.T. and Schnobrich, W.C. (1973). "Finite element analysis of reinforced concrete". *Journal of Structural Division*, ASCE, 99(10), 2109-2122.
Wang, Z.M., Kwan, A.K.H. and Chan, H.C. (1999). "Mesoscopic study of concrete I: generation of random aggregate structure and finite element mesh". *Computers and Structures*, 70(5), 533-544.
Willam, K., Pramono E. and Sture, S. (1987). "Fundamental issues of smeared crack models". *Proceedings of SEM/RILEM International Conference on Fracture of Concrete and Rock*, Houston, Texas, USA, 142-157.
Yang, Z.J. and Chen, J.F. (2005). "Finite element modelling of multiple cohesive discrete crack propagation in reinforced concrete beams". *Engineering Fracture Mechanics*, 72(14), 2280-2297.